Supplementary Text S1

Switching hybrid dynamical system

First, to consider the switching movement pattern corresponding to the external temporal input $I(t)$, a nonautonomous system (a system that depends on the external input) is defined using ordinary differential equations of the type

$$\frac{dx}{dt} = \dot{x} = f(x, I(t)), \quad x, I \in \mathbb{R}^N, \tag{S1}$$

where x and f are the state and vector field, respectively[1]. When the input $I(t)$ varies slowly in comparison to state x, the input can be regarded as a constant, resulting in a bifurcation parameter. In human movements, the finger or wrist movement corresponds to state x and regular changes in rhythm are equivalent to the input $I(t)$[2,3]. Conversely, when the change in input $I(t)$ cannot be neglected in comparison with the change in state x, it is necessary to consider how the vector fields change with time. In this case, the input is introduced as a set $\{I_l\}_{l=1}^{L}$ of temporal input I_l with finite duration T_l. For example, for the hitting movements in tennis, the temporal input with the finite duration corresponds to the forehand or backhand sides of the opponent's shot. The hitting movement pattern, state x, switches forehand and backhand strokes corresponding to the opponent's shot course. Each element of the input is defined as one period of a periodic time function. The input corresponds to a set of sampling points in a parameterized space of the function. For each sampling point, a continuous dynamical system is defined by the vector field f_l in the hyper-cylindrical phase space $\mathscr{M}$. A discrete dynamical system is defined by the iterative function g_l on the global Poincaré section Σ, which is a subspace of $\mathscr{M}$.

When the same input I_l is repeatedly fed into the system, a trajectory γ_l converges onto an attractor in the space $\mathscr{M}$[1]. This attractor is designated as an excited attractor to emphasize that it is excited by the external input. The excited attractors represent the movement pattern, such as a forehand or backhand stroke corresponding to a ball course in tennis. In general, when the external inputs are switched stochastically, a trajectory cannot converge onto both excited attractors. However, the following results have been demonstrated both analytically and numerically[4,5]. A trajectory $\gamma_l(C)$ in the hyper-cylindrical space $\mathscr{M}$ converges to the set $\Gamma(C)$ starting from the initial set C on the Poincaré section Σ. Two sets, $\Gamma(C)$ and C, are the attractive and invariant sets with a fractal-like structure; they satisfy the following equations:

$$\Gamma(C) = \bigcup_{l=1}^{L} \gamma_l(C), \tag{S2}$$

$$C = \bigcup_{l=1}^{L} g_l(C). \tag{S3}$$

The trajectory set $\Gamma(C)$ corresponding to the input set $\{I_l\}_{l=1}^{L}$ is obtained from the union of the trajectory set $\gamma_l(C)$ with each input I_l and is composed of transient trajectories between the excited attractors. The initial set C on the Poincaré section Σ is obtained from the union of the sets $\{g_l\}_{l=1}^{L}$ of iterated functions g_l on the Poincaré section[6,7]. Because the boundary between these transient trajectories is fractal, we can refer to fractal transitions between the two attractors[4].

Subsequently, the proposed integrated model is the switching hybrid dynamical system[8,9]. Here, we assume a system with a higher and lower module that interact with each other by a switching input $I_l(t)$ from the higher to lower module and by a feedback signal $x(t)$ from the lower to higher module. In addition, an external input $I_{ext}(t)$ feeds into the higher module, as shown in Supplementary Fig. S1. Here, the higher module corresponds to the brain or prefrontal cortex as the discrete dynamical system[10,11]; the higher module transforms both the external input pattern $I_{ext}(t)$ and feedback signal $x(t)$ into the input pattern $I_l(t)$. The lower module corresponds to the human motor system as the continuous dynamical system described by Eq. (S1).

Supplementary Text S2

Overview of international and collegiate matches

To capture the differences between international and collegiate matches, the final shots of a rally were categorized into winner or error: winner is a shot that is not returned by the opponent, resulting in winning a point, and error is a shot that lands incorrectly in the opponent's court, resulting in the loss of a point. A histogram of the number of rallies in each successive shot was calculated to extract the characteristics of the rallies performed by international players. Because of the characteristics of soft tennis, the length of the rally tends to be high due to the soft and light material of the ball. The high number of shots in a rally is more salient in international matches compared with collegiate matches because the ball significantly slower than that in regular tennis. Additionally, the number of errors would be lower in the international matches; therefore, the international players would need more shots to win a point than the collegiate players.

Figure S2 shows the ratio of the frequencies of a rally with lengths of 0-20 shots to the total of 314 points in international matches and 280 points in collegiate matches. The median number of rallies was six and four in international and collegiate matches, respectively.

Additionally, in the international matches, the percentages of winners and errors were 24 % and 76 % respectively; however, in rallies that included over nine shots, the percentages decreased to 13 % and 24 %, respectively. In the collegiate matches, the percentage of winners and errors was 20 % and 80 %, respectively. These ratios were similar to those for international matches; however, in rallies including over nine shots, the percentages decreased greatly to 4 % and 7 %, respectively.

The distribution patterns of the winners and errors in each short i.e., including eight or less successive shots) and long rally (i.e., including nine or more successive shots) were significantly different between the international and collegiate matches ($\chi^2(3) = 48.97, p = 1.33 \times 10^{-10}$). As the result of the residual analysis revealed, a significant skill-level difference in the error frequency was found in both the short and long rallies, whereas the difference in the number of winners was only found in the long rallies. In the short rallies, the number of errors was the highest in the collegiate matches; however, in long rallies, errors occurred most frequently in the international matches. The ratio of winners and errors in each short and long rally were similar between international and collegiate matches; in short rallies, the ratios of errors in international and collegiate matches were 0.80 and 0.82, respectively. In long rallies, the ratios of errors in international and collegiate matches were 0.68 and 0.63, respectively. This suggests that the number of errors depends on the rally length. Additionally, winners were most frequently observed in the international matches. Most of the collegiate players' rallies were short, and they made more errors in short rallies than the international players. Conversely, most of the international players' rallies were long, and in long rallies, there were more errors and winners compared with collegiate players. Thus, the skill-level difference between international and collegiate players manifests in the difference in rally length, and one of the characteristics of soft tennis skill depends on whether a rally extends beyond a certain length, for example, rallies having over nine shots.

Supplementary Text S3

Soft tennis

Soft tennis is a type of tennis that was developed in Japan from regular tennis. There are some common aspects between soft and regular tennis, but there are also some differences. The most distinctive difference is the use of rubber balls, which are much softer than the balls used in regular tennis; hence the name "soft tennis." Moreover, unique techniques and game maneuvering are required because of the softness of the ball[12]. Because only four games are necessary to win a match, the game is much shorter than regular tennis. However, the number of shots in a soft tennis rally is more than that in regular tennis because the ball velocity after a bounce decreases due to the distortion of the ball from the bounce in soft tennis[13].

Supplementary Figure S1

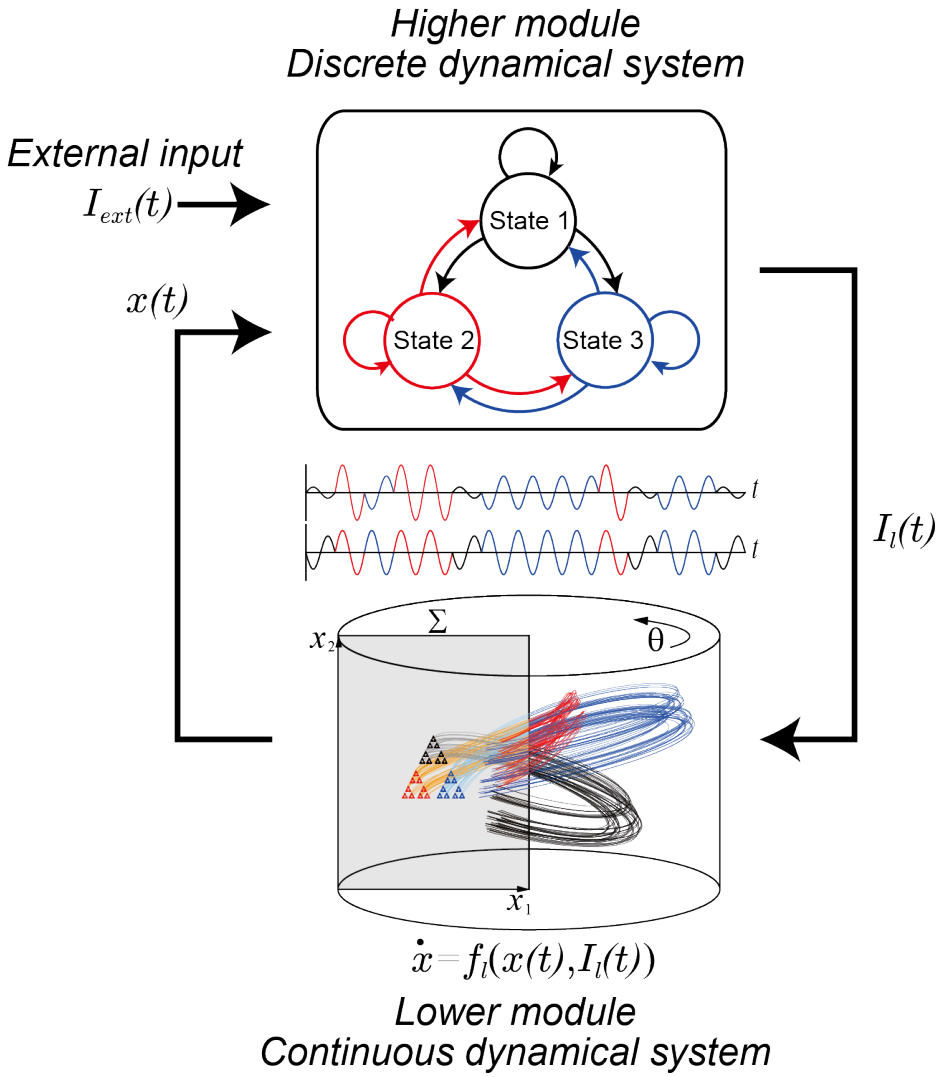

Figure S1. Schematic representation of switching hybrid dynamics composed of a discrete dynamical system as the higher module and a continuous dynamical system as the lower module with a feedback loop. This system is non-autonomous.

Supplementary Figure S2

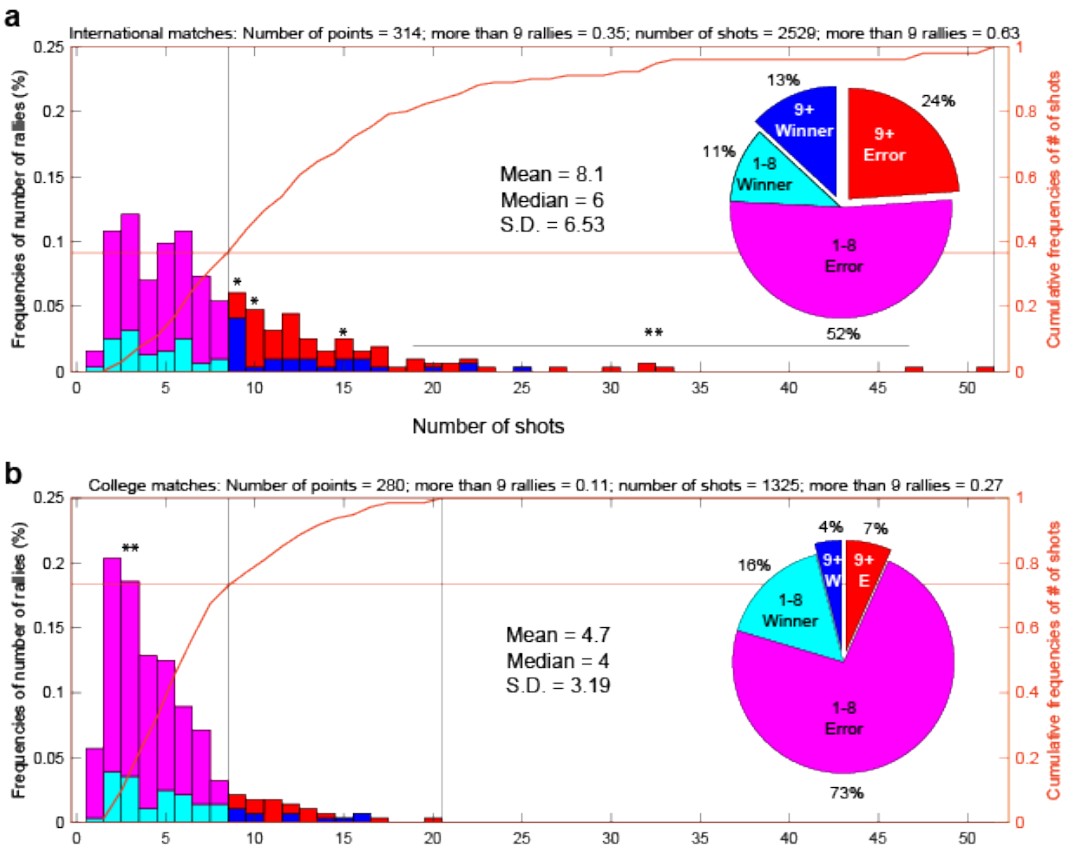

Figure S2. Frequencies of number of rallies and ratios of winners and errors. (**a**) and (**b**) show international and collegiate matches, respectively. Blue bars show the frequency of winners in rallies with over nine shots, cyan bars show the frequency of winners in rallies with less than nine shots, red bars show the frequency of errors in rallies with over nine shots, and magenta bars show the frequency of errors in rallies with less than nine shots. The orange curves show the cumulative frequencies of number of shots (right axis). The pie charts show the proportion of winners and errors for all points.

Supplementary Figure S3

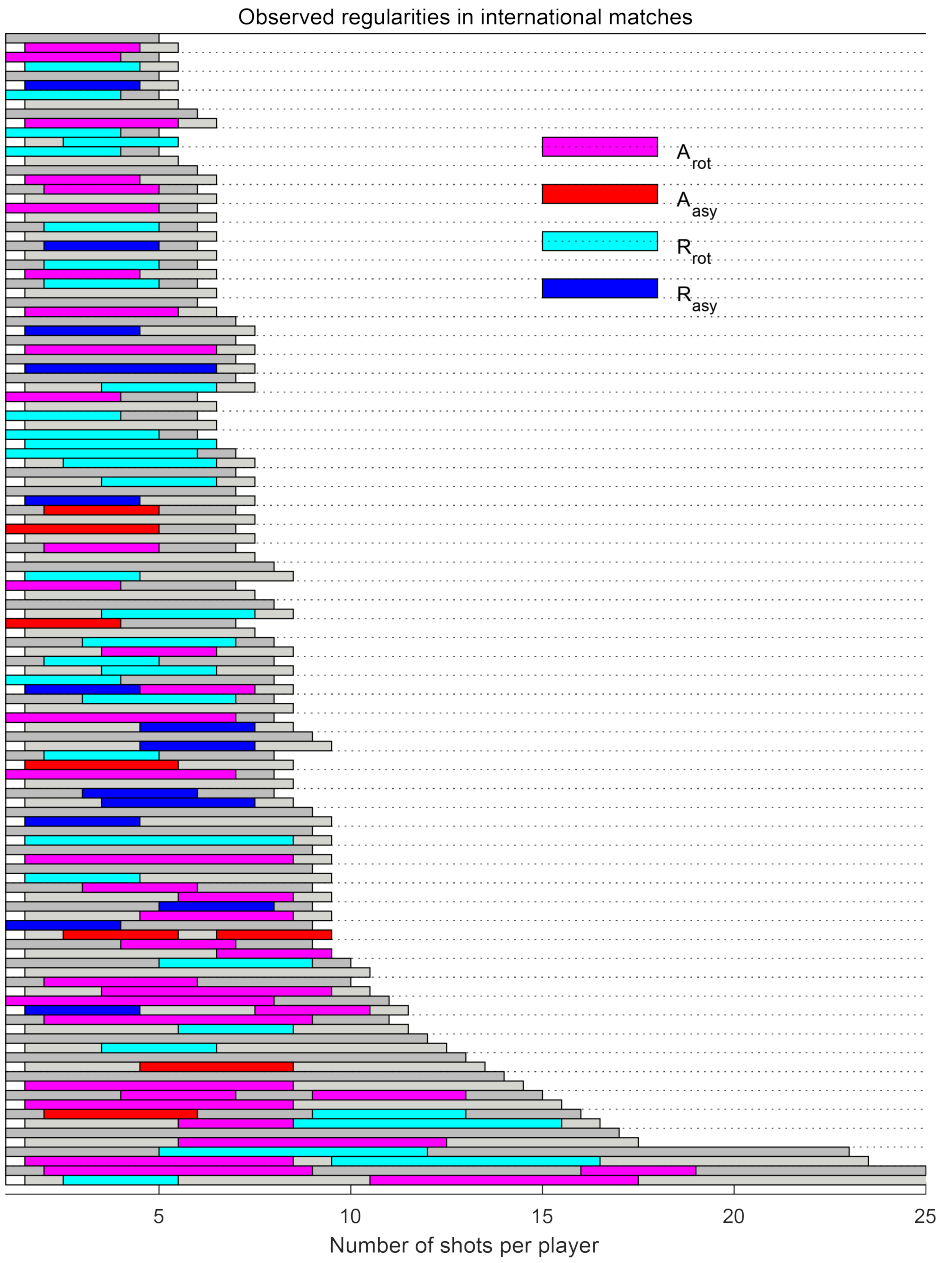

Figure S3. Observed regularities in each rally per player in international matches.

Supplementary Figure S4

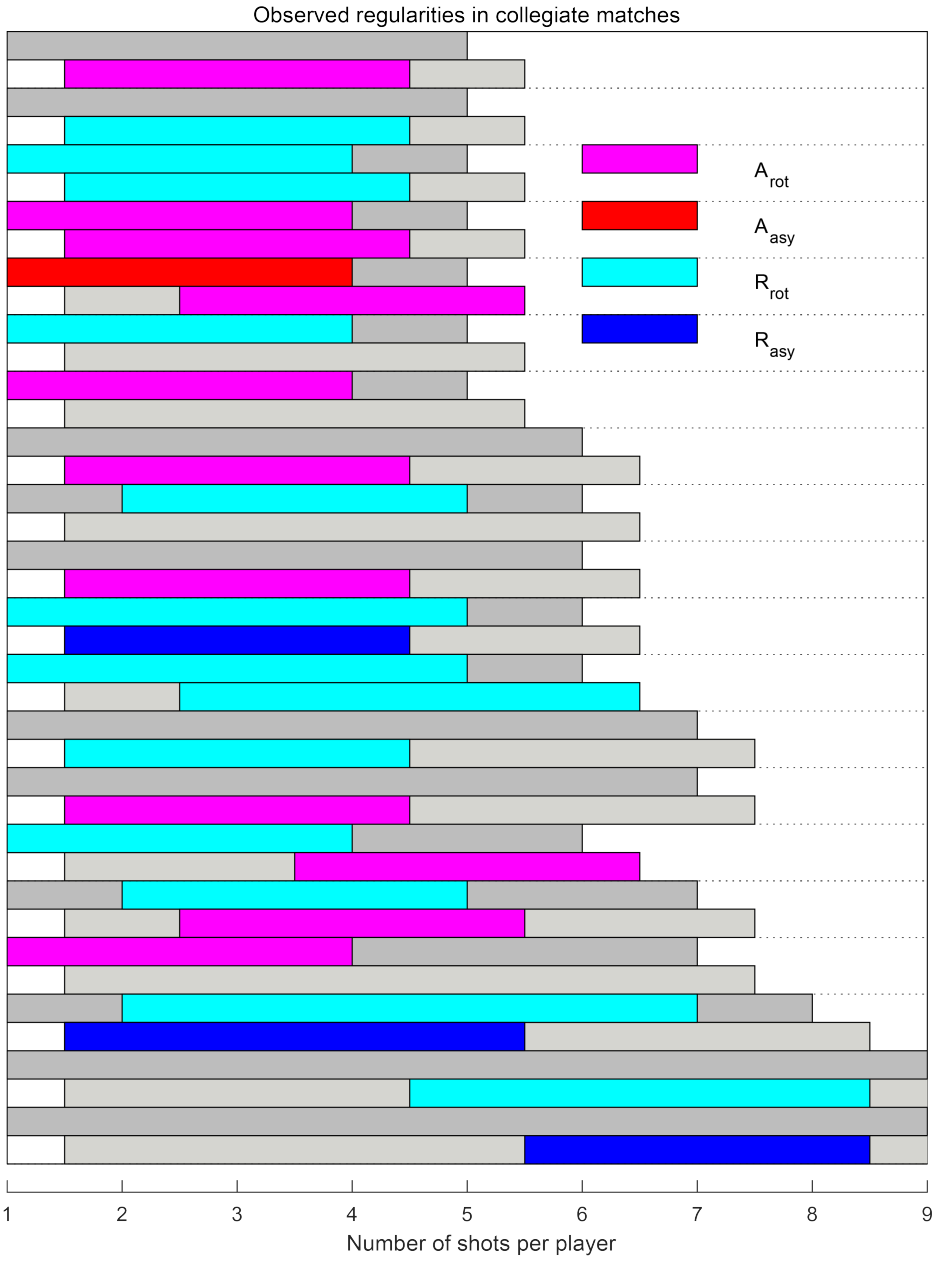

Figure S4. Observed regularities in each rally per player in collegiate matches.

Supplementary Figure S5

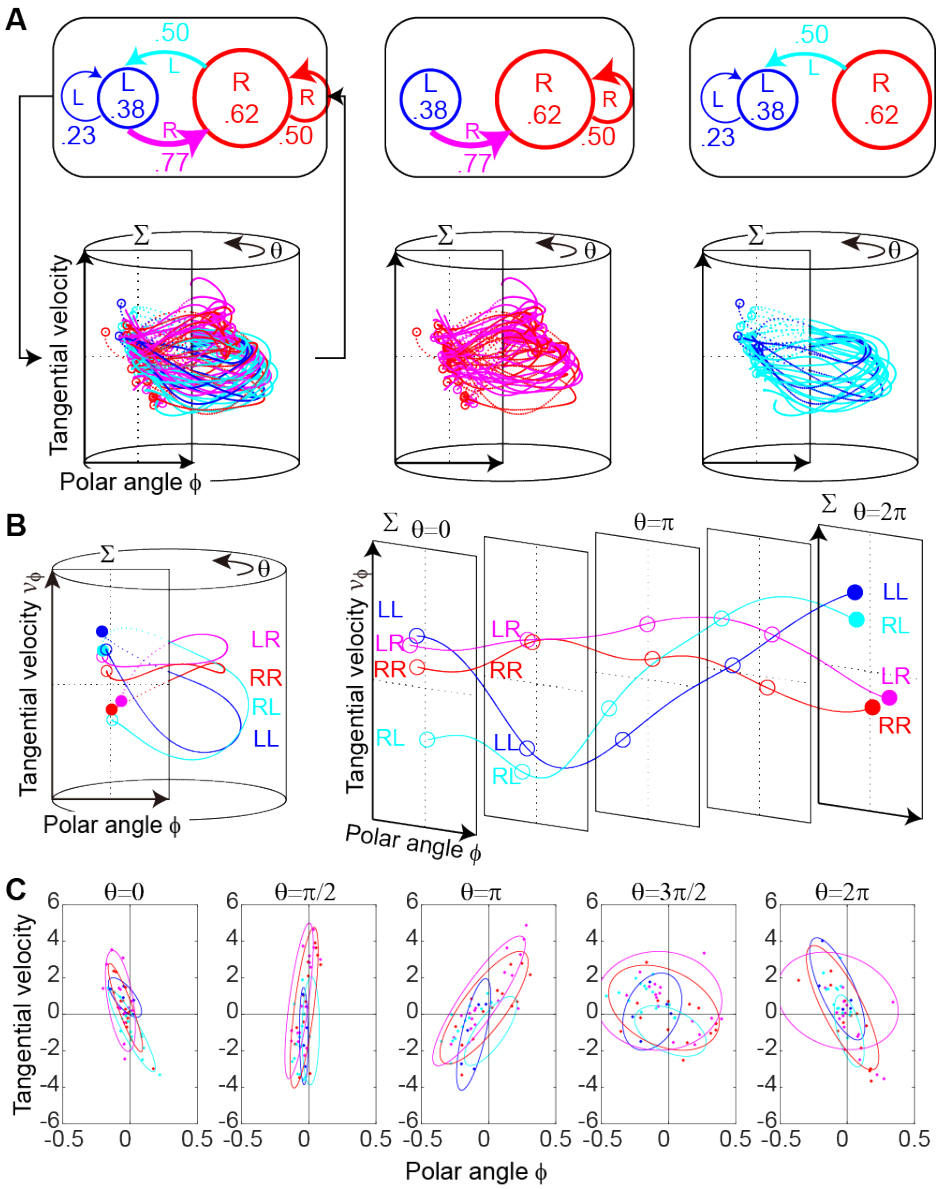

Figure S5. Switching hybrid dynamics in a collegiate match. A shows the switching hybrid system with discrete transition probabilities as the higher module and the connected continuous trajectories in cylindrical phase space as the lower module. B shows the mean trajectories expanded into the two-dimensional plane, using $\theta - (x_1, x_2)$ for switching input corresponding to panel A. The trajectories are separated corresponding to the third-order sequence effect. C shows five Poincaré sections Σ, i.e., $\theta = 0, \pi/2, \pi, 3\pi/2,$, and 2π corresponding to panel B with 80% equal probability ellipses.

Supplementary Figure S6

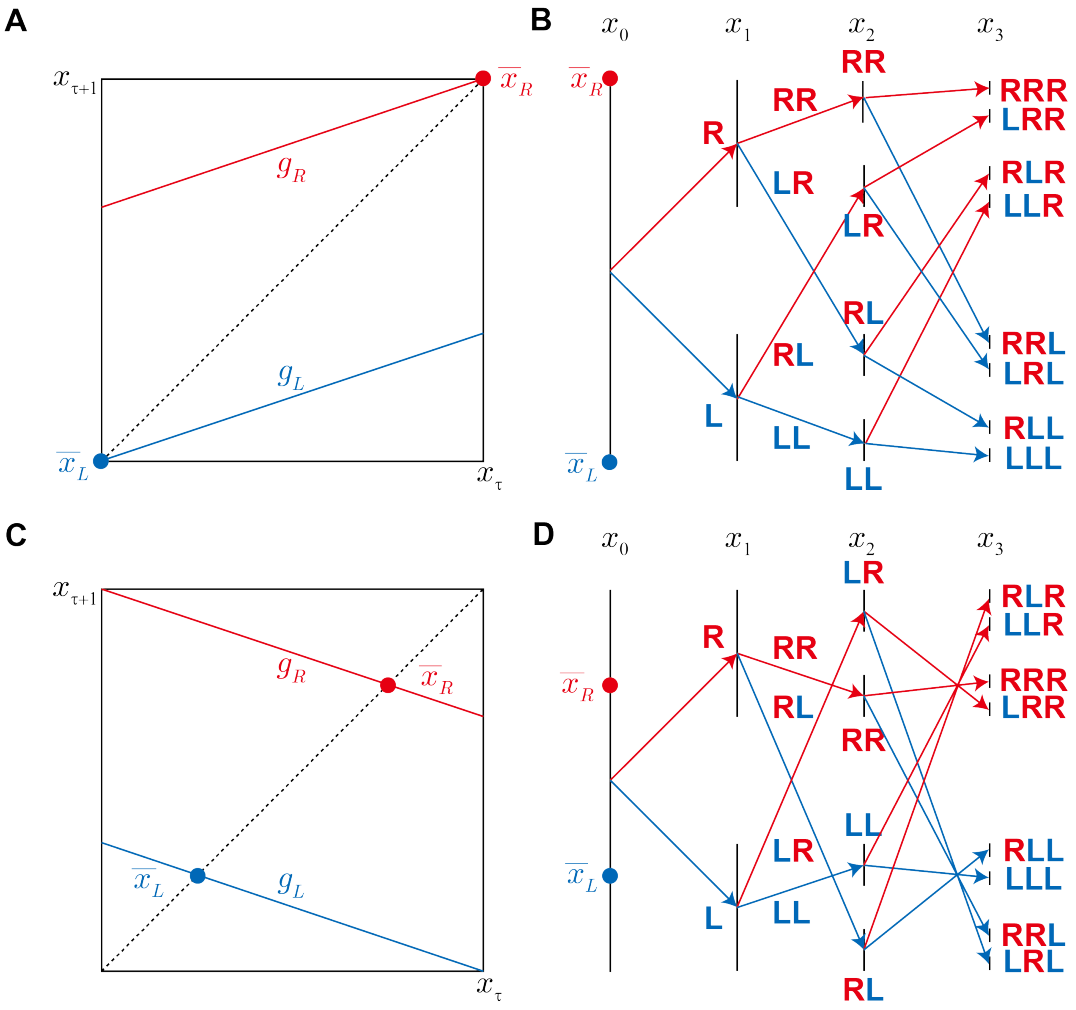

Figure S6. Hierarchical fractal structure. This demonstrates how the Cantor set can be constructed using two iterative functions. A and C show the iterative function g_R and g_L transform state x_τ to the next state $x_{\tau+1}$. In A, the lower-left and upper-right corners are the attractive fixed points $\bar{x}_L$ for g_L and $\bar{x}_R$ for g_R, respectively. B and D show the hierarchical structure of the fractal corresponding to the sequence of right (R) and left (L) side inputs from x_0 to x_3. C and D are the same as A and B, except that the transformations of iterative function g_R and g_L are rotated around the fixed points $\bar{x}_R$ and $\bar{x}_L$, respectively. We named this the Cantor set with rotation.

Supplementary Figure S7

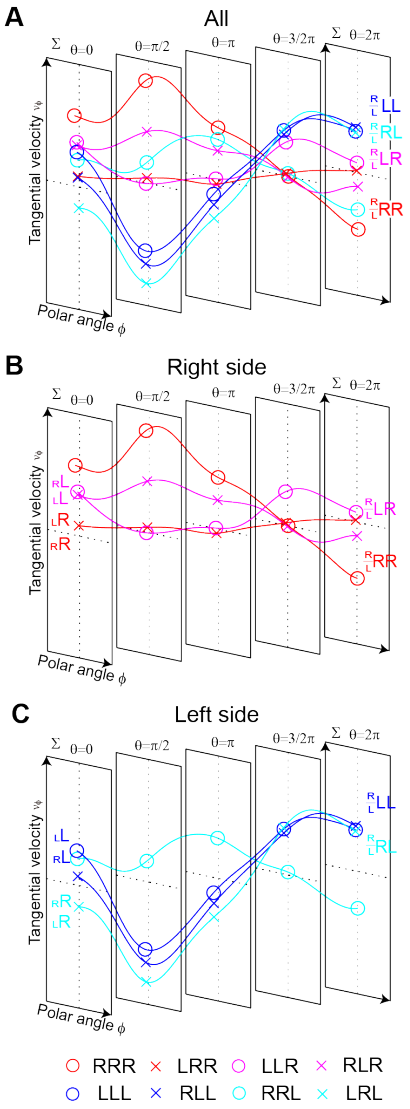

Figure S7. Eight trajectories of transitions between two excited attractors. The mean trajectories are expanded into the two-dimensional plane, using $\theta - (x_1, x_2)$ as the switching input. The trajectories are drawn using the third-order sequence effect. A shows eight mean trajectories. B and C show four mean trajectories corresponding to right and left side inputs, respectively.

Supplementary Figure S8

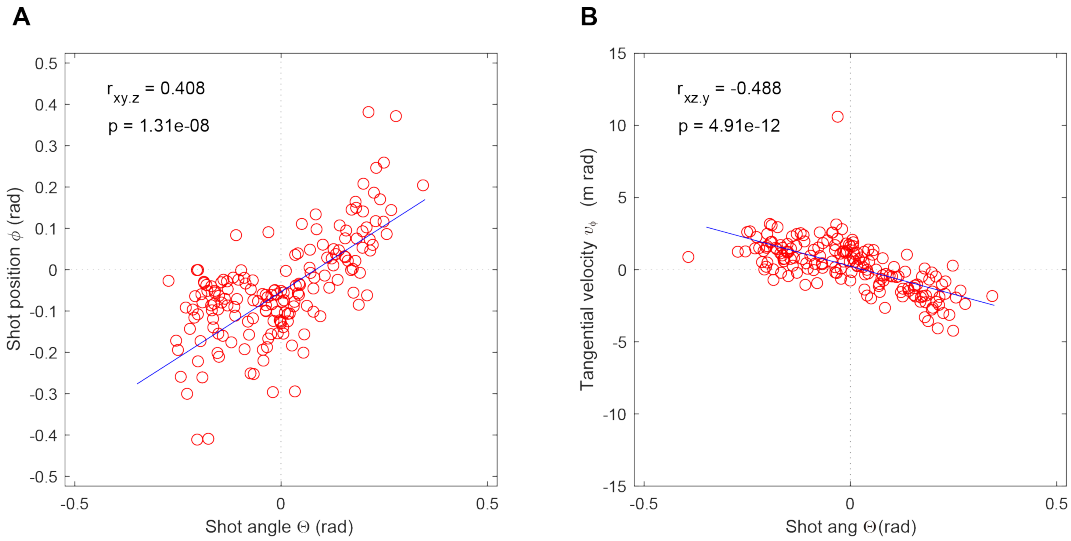

Figure S8. Partial correlation. A shows the partial correlation between the shot angle Θ and polar angle ϕ. B shows the partial correlation between the shot angle Θ and tangential velocity v_ϕ.

Supplementary Figure S3

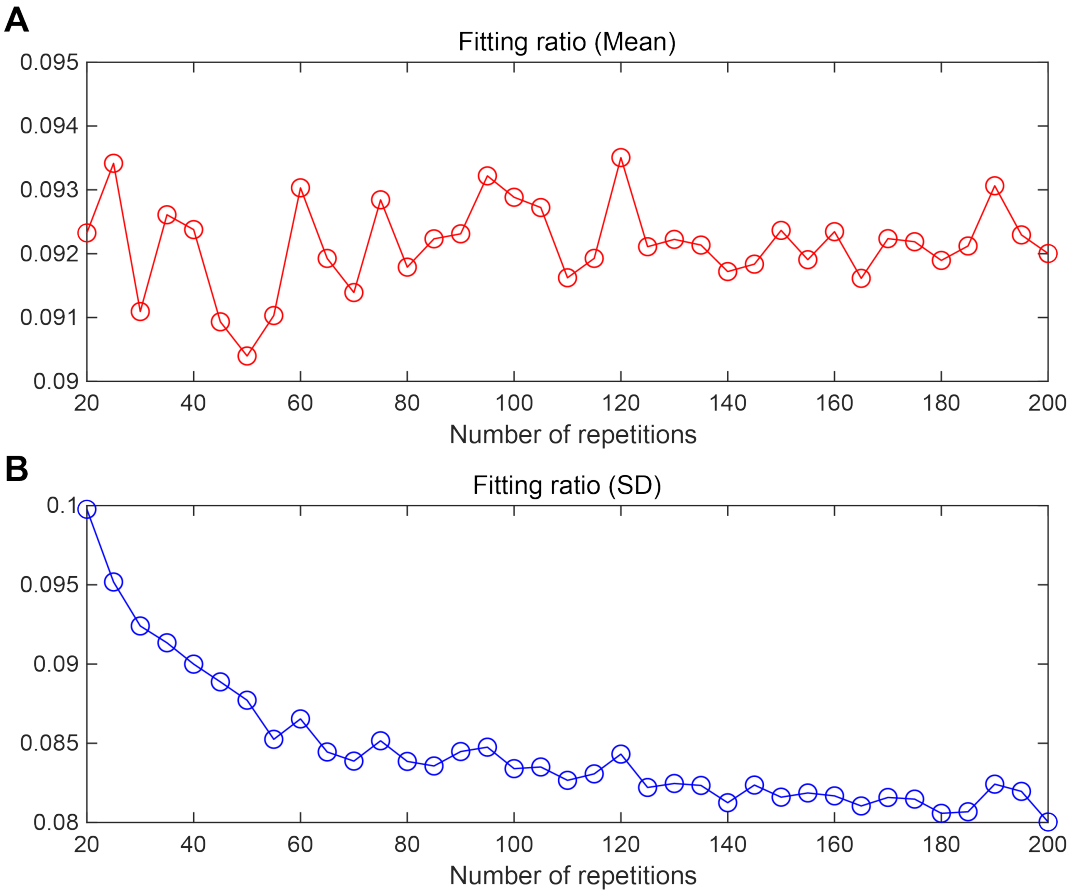

Figure S9. Means and standard deviations (SDs) of the fitting ratio by the number of random shuffling repetitions for surrogate data. A shows the change in mean of the fitting ratio for 20–200 repetitions. B shows the change in SD of the fitting ratio for 20–200 repetitions.

Supplementary Figure S10

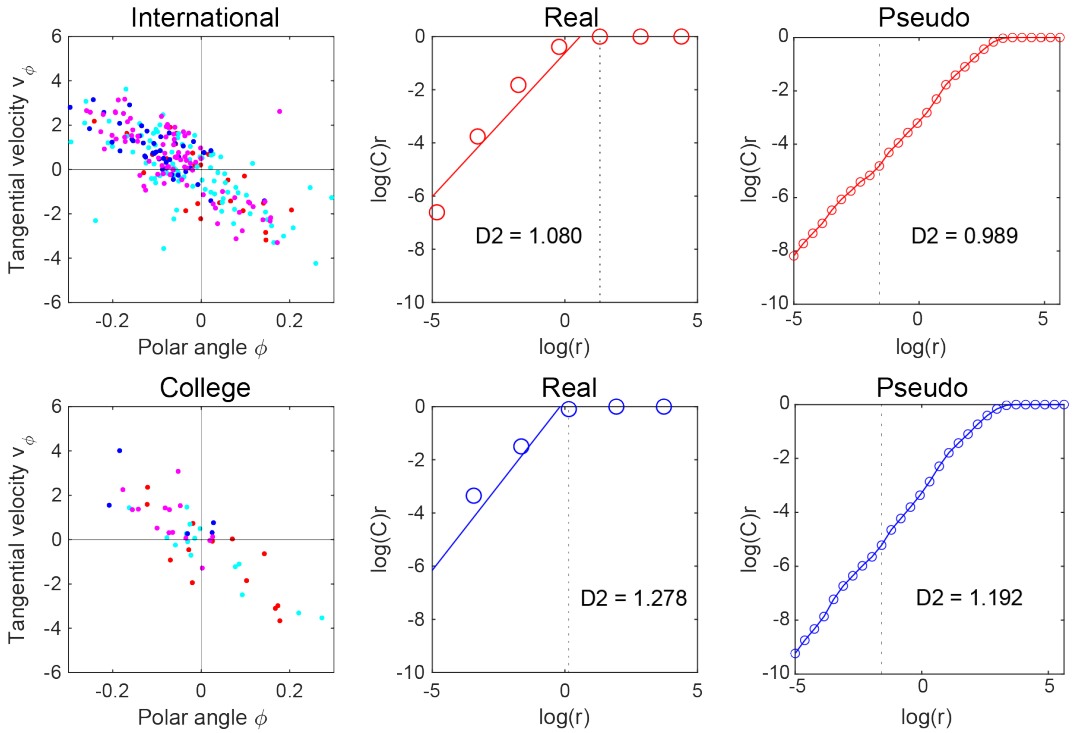

Figure S10. Poincaré maps for the international (A) and collegiate (B) matches and correlation dimensions for both matches (C).

Supplementary Figure S11

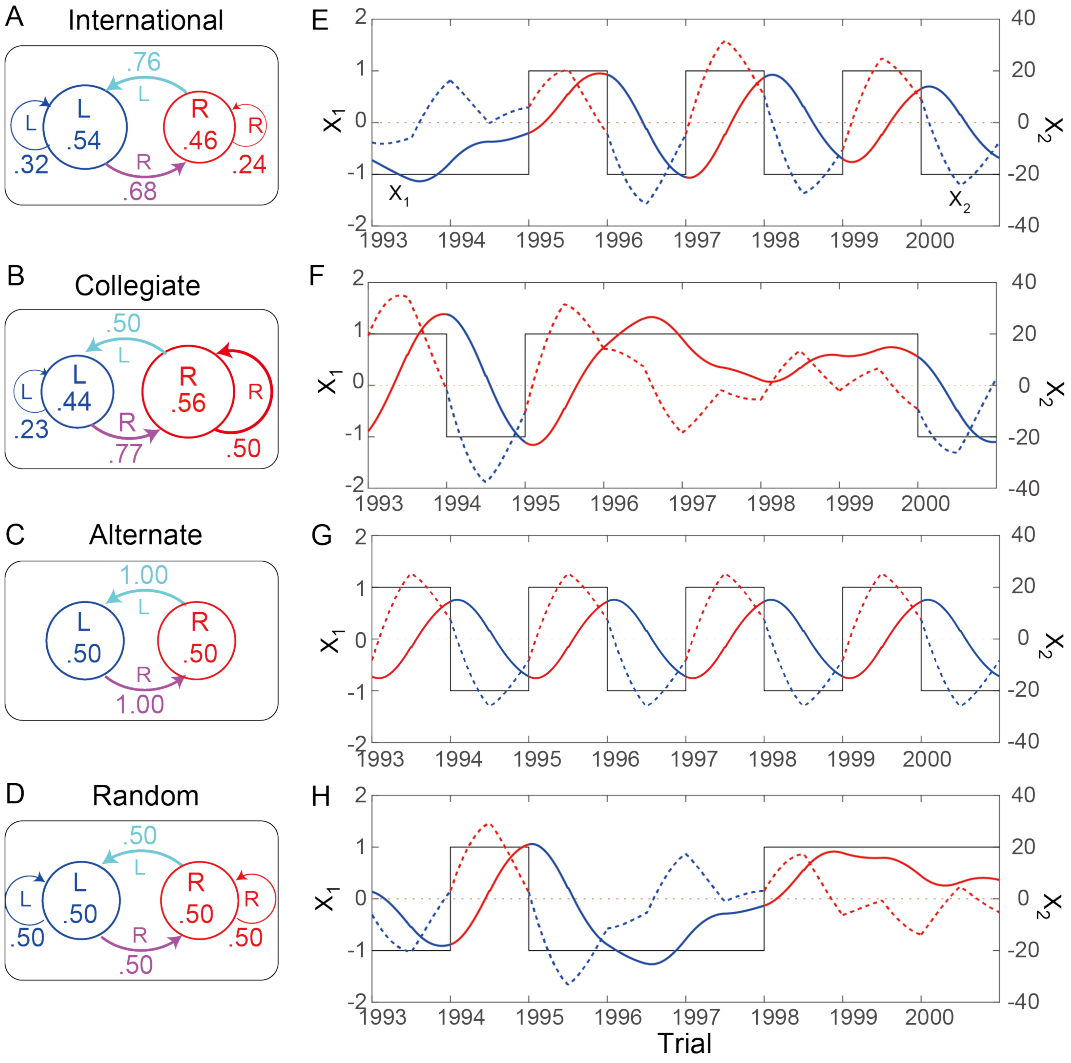

Figure S11. State transition probabilities for the simulation experiment and examples of results. A to D show the second-order state transition probabilities for the pseudo-international, alternate, and random series, respectively. E to H show examples of the results of the simulation experiments corresponding to A to D, respectively. The black step waves show the external input pattern, red and blue lines show the output pattern for x_1, and red and blue dotted lines show the output pattern for x_2.

Supplementary Movie M1

Typical example of well-fitted rally in international matches corresponding to Figure 4.

References

1. Gohara, K. & Okuyama, A. Dynamical systems excited by temporal inputs: Fractal transition between excited attractors. *Fractals* **7**, 205–220, DOI: https://doi.org/10.1142/S0218348X99000220 (1999).
2. Kelso, J. A. S. Phase transitions and critical behavior in human bimanual coordination. *Am. J. Physiol.* **246**, R1000–R1004, DOI: https://doi.org/10.1152/ajpregu.1984.246.6.R1000 (1984).
3. Haken, H., Kelso, J. A. S. & Bunz, H. A theoretical model of phase transitions in human hand movements. *Biol. Cybern.* **51**, 347–356, DOI: https://doi.org/10.1007/BF00336922 (1985).
4. Gohara, K. & Okuyama, A. Fractal transition: Hierarchical structure and noise effect. *Fractals* **7**, 313–326, DOI: https://doi.org/10.1142/S0218348X99000311 (1999).
5. Yamamoto, Y. & Gohara, K. Continuous hitting movements modeled from the perspective of dynamical systems with temporal input. *Hum. Mov. Sci.* **19**, 341–371, DOI: https://doi.org/10.1016/S0167-9457(00)00018-X (2000).
6. Hutchinson, J. E. Fractals and self similarity. *Indiana Univ. Math. J.* **30**, 713–747 (1981).
7. Barnsley, M. F. *Fractals everywhere* (Academic Press, San Diego, CA, 1993), 2nd edn.
8. Nishikawa, J. & Gohara, K. Automata on fractal sets observed in hybrid dynamical systems. *Int. J. Bifurc. Chaos* **18**, 3665–3678, DOI: https://doi.org/10.1142/S0218127408022639 (2008).
9. Nishikawa, J. & Gohara, K. Anomaly of fractal dimensions observed in stochastically switched systems. *Phys. Rev. E* **77**, 036210, DOI: https://doi.org/10.1103/PhysRevE.77.036210 (2008).
10. Miller, E. K. The prefrontal cortex and cognitive control. *Nat. Rev. Neurosci.* **1**, 59–65, DOI: https://doi.org/10.1038/nrn35036228 (2000).
11. Sakagami, M. & Tsutsui, K. The hierarchical organization of decision making in the primate prefrontal cortex. *Neurosci. Res.* **34**, 79–89, DOI: https://doi.org/10.1016/S0168-0102(99)00038-3 (1999).
12. Japan Soft Tennis Association. What is soft tennis. https://www.jsta.or.jp/wp-content/uploads/international/en/whats.html (2022.4.7).
13. Fitzpatrick, A., Stone, J., Choppin, S. & Kelley, J. Important performance characteristics in elite clay and grass court tennis match-play. *Int. J. Perform. Analysis Sport* **19**, 942–952, DOI: https://doi.org/10.1080/24748668.2019.1685804 (2019).